New Zealand Journal of Geology and Geophysics

ISSN: (Print) (Online) Journal homepage: https://www.tandfonline.com/loi/tnzg20

A mass transport deposit in the Permian Mackellar Formation, Victoria Group, Antarctica

David H. Elliot & John L. Isbell

To cite this article: David H. Elliot & John L. Isbell (2021): A mass transport deposit in the Permian Mackellar Formation, Victoria Group, Antarctica, New Zealand Journal of Geology and Geophysics, DOI: 10.1080/00288306.2020.1868538

To link to this article: https://doi.org/10.1080/00288306.2020.1868538

Published online: 17 Jan 2021.

NEW ZEALAND JOURNAL OF GEOLOGY AND GEOPHYSICS
https://doi.org/10.1080/00288306.2020.1868538

Taylor & Francis
Taylor & Francis Group

RESEARCH ARTICLE

A mass transport deposit in the Permian Mackellar Formation, Victoria Group, Antarctica

David H. Elliot [a] and John L. Isbell[b]

[a]School of Earth Sciences and Byrd Polar and Climate Research Center, Ohio State University, Columbus, OH, USA; [b]Department of Geosciences, University of Wisconsin- Milwaukee, Milwaukee, WI, USA

ABSTRACT

The Permian Mackellar Formation in the central Transantarctic Mountains is a fine-grained siliciclastic succession, which was deposited in a marine to brackish inland sea (Mackellar Sea) along the hinterland of the Gondwana margin. The Mackellar strata were deposited in an elongate, trough-shaped basin oriented subparallel to the present trend of the Transantarctic Mountains. At the head of the Robb Glacier, the Mackellar beds include, in the middle of the succession, a mass transport deposit, which exhibits folding and thrusting. Structural data (e.g. facing direction and axial planes of overturned folds, orientation and vergence of thrust faults) indicate axial transport down the elongate depositional basin. Unconformable relationships to strata overlying the mass transport deposit suggest reactivation and doming of the deposit following its initial emplacement. Subsequently there was partial collapse of the toe-ward part of the extant deposit along a listric fault, the result of loading by deltaic sandstones of the overlying Fairchild Formation.

ARTICLE HISTORY
Received 27 August 2020
Accepted 18 December 2020

HANDLING EDITOR
Lorna Strachan

KEYWORDS
Antarctica; Robb Glacier; Permian; Mackellar; mass transport deposit; deformation

Introduction

Mass transport deposits (MTDs or mass transport complexes, MTCs), in the form of coherent to semi-coherent to chaotic intervals of strata, are well-documented in marine successions, particularly among some basin margin successions (e.g. Ammerman et al. 2011; Dykstra et al. 2011; Ineson 1985; King et al. 2011; Macdonald et al. 1993; Moscardelli et al. 2006; Posamentier and Martinsen 2011; Posamentier and Walker 2006; Van der Merwe et al. 2009). Such deposits have been studied extensively in the Gulf of Mexico and in outcrop at several locations worldwide and spanning much of the geologic column (Shipp et al. 2011 and the references therein). Depositionally, MTDs have been noted mainly in shallow to deep-water siliciclastic systems and some have been interpreted to mark the onset of increasing sediment supply to the basin. Of particular note, however, are the exceptionally exposed upper Pleistocene deposits adjacent to the Dead Sea (Alsop et al. 2017, 2018, 2019) and the upper Carboniferous Guandacol Formation in Argentina (Sobiesiak et al. 2017). The driving force for emplacement of MTDs is commonly attributed to either gravitational effects or tectonism (e.g. Alsop et al. 2017; Posamentier and Martinsen 2011).

A slide with limited exposure, but with characteristics of some MTDs, occurs within a Permian shallow-water fine-grained succession in the Antarctic Gondwana succession (Barrett 1991; Miller and Collinson 1994; Miller and Isbell 2010). The exposed slide in the Mackellar Formation exhibits folding and en échelon thrusting of an interval with, locally, a sandstone core. It is here described and an interpretation presented.

Geologic setting

Regional geology

The Devonian to Triassic Beacon Supergroup (Barrett 1991), of which the Victoria Group is the Permo-Triassic part, is widely exposed in the Transantarctic Mountains (Figure 1). The Beacon strata overlie an erosion surface (Kukri Erosion Surface; Isbell 1999) cut across a pre-Devonian basement of igneous, metamorphic, metasedimentary and metavolcanic rocks, mainly of early Paleozoic age (Elliot 2013; Stump 1995). Devonian quartzose strata of the Taylor Group are well developed in south Victoria Land, but probable Devonian strata south of the Byrd Glacier form only scattered outcrops (Isbell 1999). A second erosion surface (Maya Erosion Surface) cuts the Devonian beds and, in places, pre-Devonian basement rocks. On this surface, the major part of the preserved Gondwana successions of Permo-Triassic age in the Transantarctic Mountains (Figure 2) was deposited (other Gondwana successions of comparatively limited extent are exposed in Queen Maud Land and the Amery Ice Shelf region).

CONTACT David H. Elliot elliot.1@osu.edu

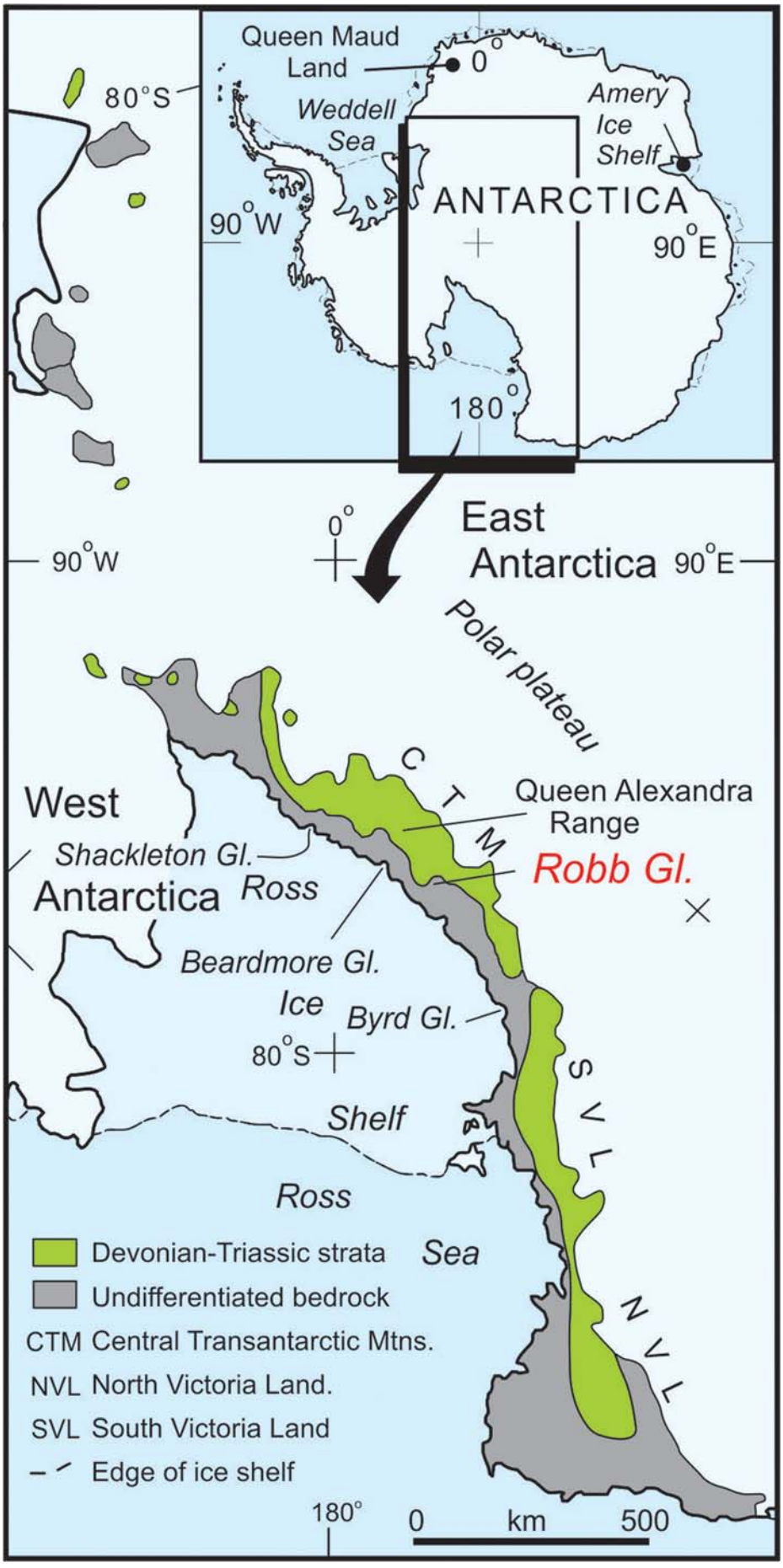

Figure 1. Location map for Antarctica.

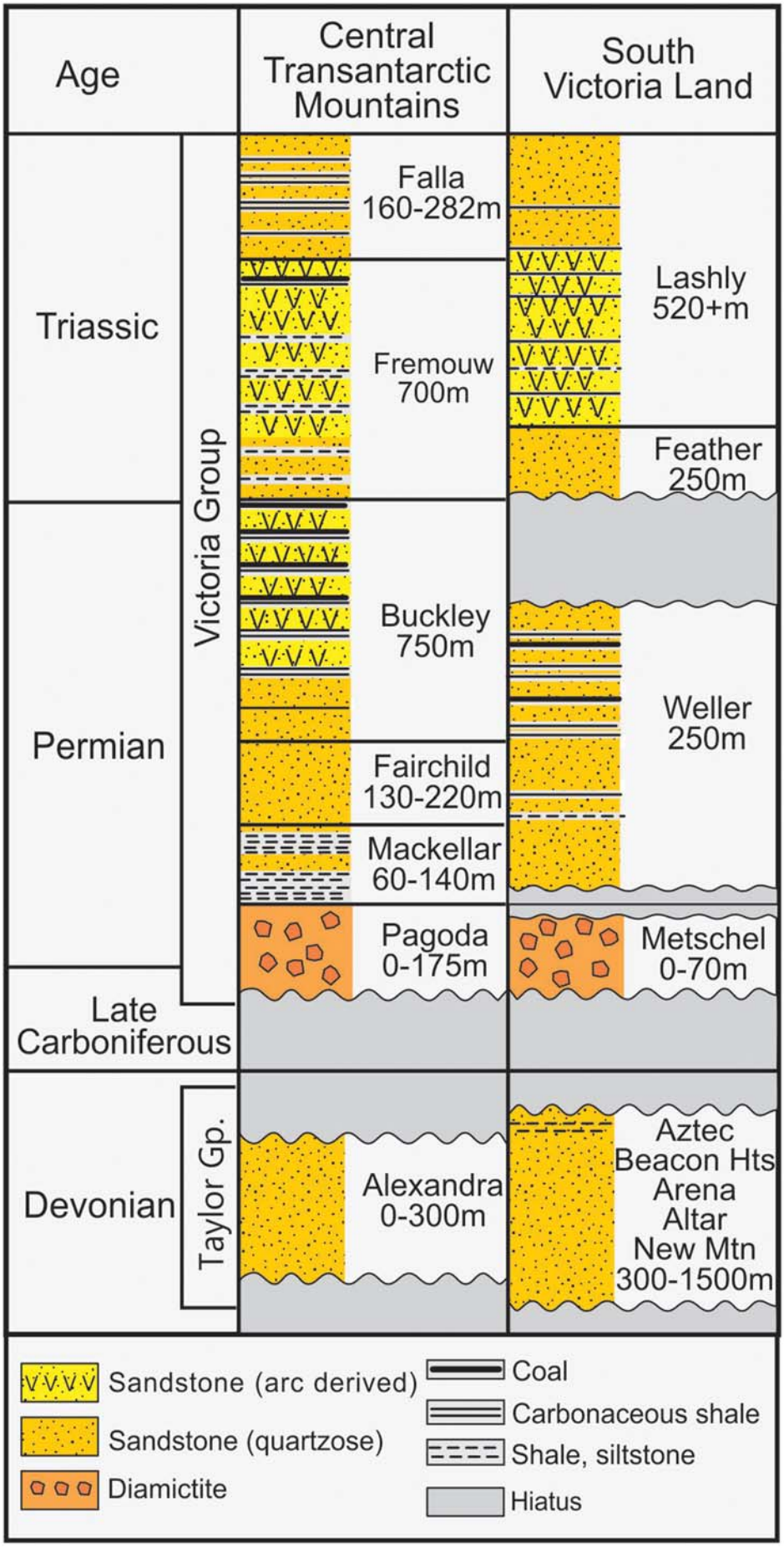

Figure 2. Stratigraphy of the Beacon Supergroup in the central Transantarctic Mountains and south Victoria Land.

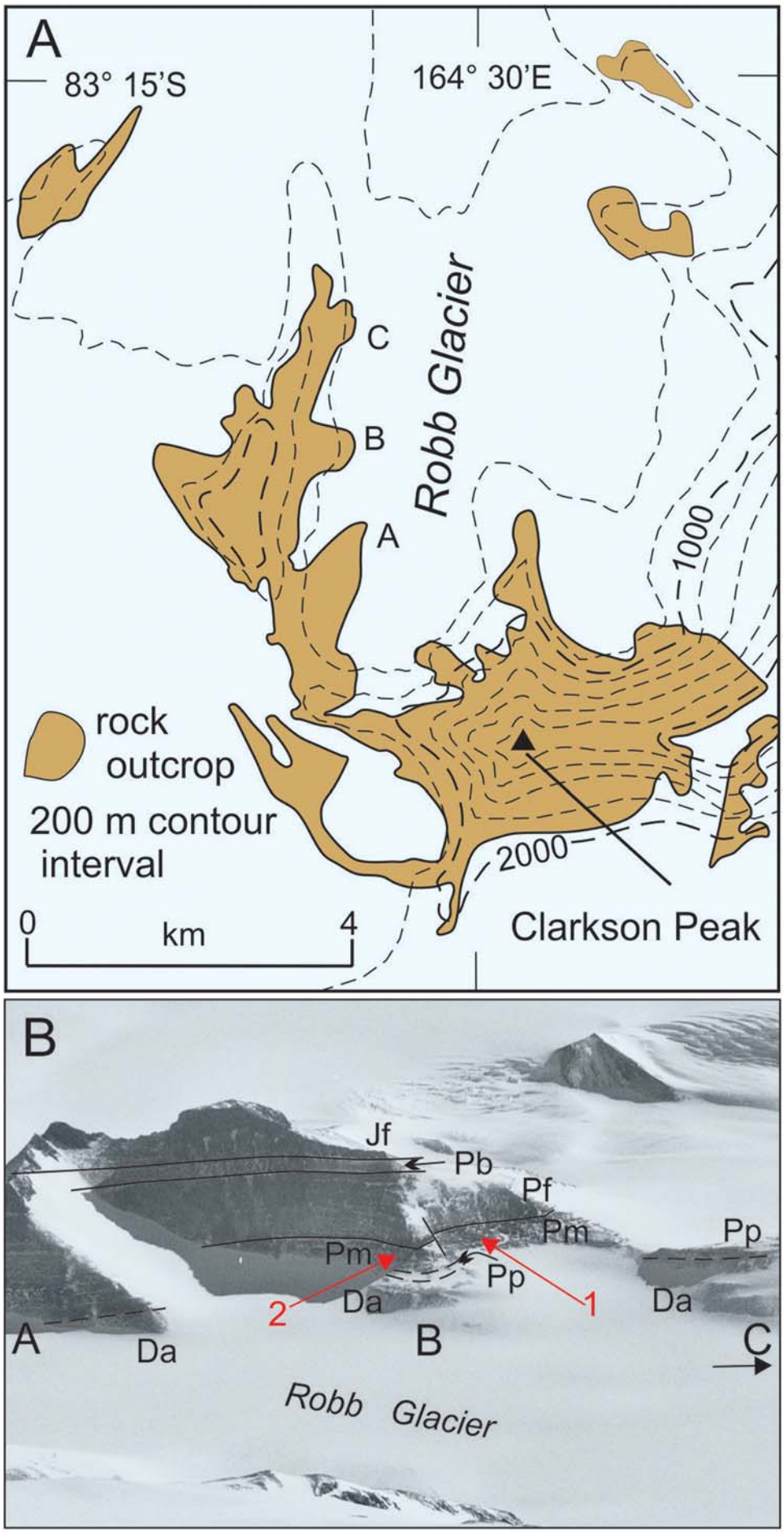

Figure 3. A, Map of the uppermost Robb Glacier region (from Barrett et al. 1970) with locations of stratigraphic sections (Figure 4) indicated by capital letters. Note that the orientation of this map is opposite to that in Figure 1. **B,** View looking west at the uppermost Robb Glacier region (modified from Polar Geospatial Center/USGS photograph CA0765 33R 0262). Red arrow #1 points to the MTD and the #2 to the face approximately parallel to the strike of the MTD. Capital letters indicate the locations of the stratigraphic sections. Da: Alexandra Fm.; Pp: Pagoda Fm.; Pm: Mackellar Fm.; Pf: Fairchild Fm.; Pb: Buckley Fm.; Jf: Ferrar dolerite.

The Permo-Triassic Gondwana succession is most fully developed in the central Transantarctic Mountains (CTM) (Figure 2). Pre-Permian beds (probably Devonian in age) have been identified in a few localities (e.g. Barrett et al. 1986; Laird et al. 1971), but many stratigraphic successions begin with Permian glacial beds (Pagoda Formation), which pass up into post-glacial shales and fine-grained, thin-bedded sandstones of the Mackellar Formation. The Mackellar Formation is overlain by deltaic beds of the Fairchild Formation, which is succeeded by fluvial coal-bearing strata of the Permian Buckley Formation. Triassic strata (Fremouw and Falla formations) are also fluvial and to a lesser extent coal-bearing. In detail, the Victoria Group in the CTM differs from that in south Victoria Land (SVL) (Figure 2). In particular, in SVL there is no equivalent of the Mackellar Formation, and coal-bearing beds of the Weller Formation, for the most part, are disconformable on the Metschel Tillite, although locally are demonstrably conformable.

The Mackellar Formation is interpreted as the filling of a very extensive, shallow, marine to brackish inland sea, the Mackellar Sea (Miller and Collinson 1994; Miller and Isbell 2010), which had developed on glaciomarine deposits of the Pagoda Formation (Isbell et al. 2008) following collapse of the Permian ice sheets. The tectonic setting of the Pagoda strata is interpreted to be a fault-bounded rift basin (Collinson et al. 1994; Isbell 2015; Isbell et al. 1997, 2008), and the paleocurrent orientations and paleoenvironments of the Mackellar beds likewise suggest deposition in an elongate narrow basin.

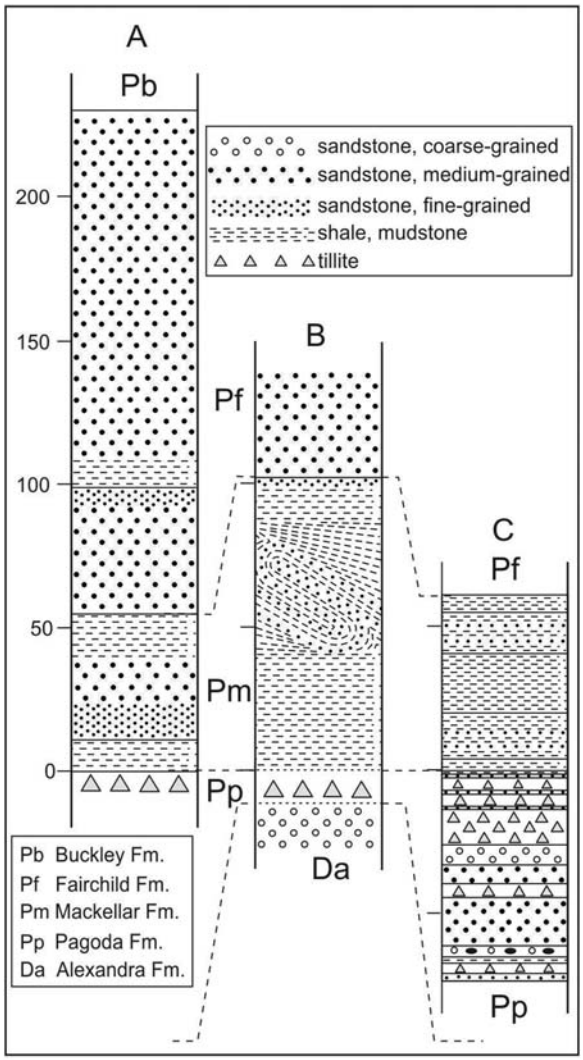

Figure 4. Stratigraphic columns for the Mackellar Formation and adjacent rock units in the upper Robb Glacier region. Locations given in Figure 3. Columns A and C from Barrett et al. (1986).

Stratigraphy at the head of the Robb Glacier

Two stratigraphic sections were measured by previous investigators in the vicinity of the uppermost Robb Glacier (Figures 1, 3), northwest of Clarkson Peak. One measured by P.J. Barrett (1968) is located on the far southernmost promontory on the west side of that glacier (site A, Figure 3A), and the other by J.F. Lindsay (Barrett et al. 1986) lies 3 km to the north (site C, Figure 3A). At the former site the measured section (Figure 4, column A) comprises a few m of the top of the Pagoda Formation (pebbly sandstone grading into shale), 55 m of bedded fine-grained sandstones and shales of the Mackellar Formation, and, above an erosion surface, 175 m of fine to medium sandstones of the Fairchild Formation (Barrett et al. 1986, Plate 1b, section Z3). At the latter site (Barrett et al. 1986, Plate1a, section L), where the upper contact of the Devonian(?) Alexandra Formation is obscure, 160 m of Pagoda Formation comprising tillite, sandstone and sparse conglomerate are overlain by 62 m of Mackellar beds (Figure 4, column C). These consist of laminated and very fissile shales with interbedded intervals of mudstone and sandstone.

The MTD locality lies between the sections just described. At this locality (Figure 3A, site B; Figure 4, column B), the uppermost 13 m of the quartzose Alexandra Formation of presumed Devonian age form the lowest exposed outcrops. Pagoda Formation glacial beds have been identified only as scattered remnants on the Maya Erosion Surface, which is the upper bounding surface of the Alexandra Formation. The Maya surface has a cover of assorted surficial debris, which is probably of late Cenozoic glacial origin. In scattered places lithified till, presumed to be Pagoda glacigenic beds, is exposed in windows through the cover. The thickness of Pagoda beds is uncertain but must be small and not exceeding about 5 m. Surface debris covers any preserved contact between the Pagoda and Mackellar formations. The 160-m-thickness of Pagoda Formation (Figure 4, column C) measured

about 1 km to the north of the slide locality demonstrates that significant local paleotopography must exist on the Maya Erosion Surface. From scattered outcrops throughout the central Transantarctic Mountains, there is evidence for even greater relief on this surface (Barrett et al. 1986; Isbell 1999).

At the MTD locality (Figure 5), the post-glacial Mackellar Formation comprises shales, siltstones and fine- to medium-grained sandstones with a thickness in outcrop of about 100 m (this includes duplication of section caused by thrusting and folding). The MTD is embedded in the Mackellar Formation, such that intervals of undeformed shaley beds both underlie and overlie the MTD itself. The uppermost Mackellar beds are slightly coarser grained and are interbedded with sandstones, forming a transition zone into the Fairchild Formation. For descriptive purposes, the base of the Fairchild Formation is arbitrarily placed at the lowest, intact, continuous cliff-forming series of sandstone beds (see later).

The MTD is exposed principally on the east face of a N-S trending ridge (Figure 3B). Immediately to the south, poorly exposed Mackellar strata occur beneath Fairchild beds at the base of a northeast-trending face (in shadow on Figure 3B). The Mackellar section has a c. 8° dip to the west, measured on slightly more resistant beds toward the northern end of the outcrop belt, but these beds are regarded as slumped because of variable attitudes. Structure contours on the Beacon-basement contact suggesta regional dip of about 3° to the west (Barrett et al. 1970), which is more consistent with the structural analysis of the MTD rocks (see later) and implies slight rotation (slumping) of the poorly lithified outcrops, below the MTD, on which the attitudes were measured.

Mass transport deposit

The Mackellar Formation, dominated by shale and mudstone, forms recessive slopes. A panoramic view of the outcrop from the east is shown in Figure 5. From the north (right end in lower half of that figure), the MTD emerges from a talus slope, which has little or no outcrop, as a series of slightly overlapping sheets of more resistant strata up to about five metres thick. Southward, beds within individual thrust sheets are variously folded, and the thrust sheets steepen and gain elevation before being lost in a major talus slope that obscures both the overlying basal Fairchild beds and the Mackellar strata. The talus slope conceals a fault, down to the south. To the south of this talus slope, the extant structure is represented by thrust sheets (each no more than about two metres thick) and very sparse folded strata (with amplitudes no more than about two metres), but it is then lost beneath surficial debris as the topography swings from an east-facing slope to a southeast-facing slope.

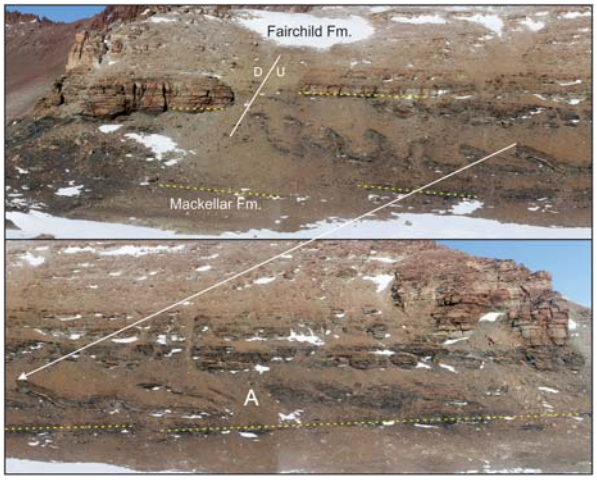

Figure 5. Panorama, looking west, of the mass transport deposit. The two images are linked by the white arrow. Bedding in the Mackellar Formation toward the base of the formation and the upper contact are indicated by the dashed yellow lines.

North of the fault zone

The exposed outcrop length of the MTD north of the fault is about 450 m. The MTD rocks exposed at the northern part of this outcrop form a series of overlapping thrust sheets each about two metres thick. At point A in Figure 5, there is a break in the MTD outcrop and to the south it forms a series of thrust sheets, which exhibit folded strata. Eleven thrusts have been identified within this part of the structure (Figure 6) although others to the north of thrust #11 may be concealed beneath talus. The exposed part of the structure north of the fault zone suggests a minimum of about 30% shortening of its original length, based in part on the sandstone bed within several thrust sheets and omitting any layer-parallel shortening that might have preceded thrusting (Alsop et al. 2017).

Figure 6. Panorama, looking west, of the mass transport deposit north of the fault. Approximate positions of thrusts, separating individual thrust sheets (numbered in black), are indicated by white arrows. Folded strata are clear in thrust sheets #1, 2, 3, 4 and 6 (indicated by dashed yellow lines). Bedding in Mackellar strata indicated by dashed yellow lines. Mackellar-Fairchild contact indicated by solid yellow line. Note the apparent unconformity between the two formations above thrust sheet #4 (sites 24, 25). Locations of sites mentioned in the text and figure captions are indicated by white numbers.

Figure 7. Hinge of synclinal fold in thrust sheet #2 (site 18, Figure 6). Shaley beds above the resistant sandstone are broken and sheared, and the dashed white line marks the approximate location of the bounding thrust between sheets #2 and 3.

To the south of Point A (Figure 5), the thrusts cut through original folds, which most probably had small amplitudes (Figure 7). With one exception (sheet #4), overturned limbs have not been identified. This sequence of thrusts, with increasingly steep attitudes southward, vanishes in the fault zone. The vergence of the thrusts and folds is toward the south. The thickness of the Mackellar section increases toward the fault, because of folding and ramping and the duplication of beds.

Within some thrust sheets (#1, 2, 3, 4, 6) a more resistant sandstone bed displays the folding. Small-scale S-folds and Z-folds are present in some thin-bedded shales and fine-grained sandstones (Figure 8A, B; Figure 9A). Cleavage is developed in many of the shale beds and in some it is demonstrably an axial plane cleavage (Figure 9A, B). Cleavage, in a

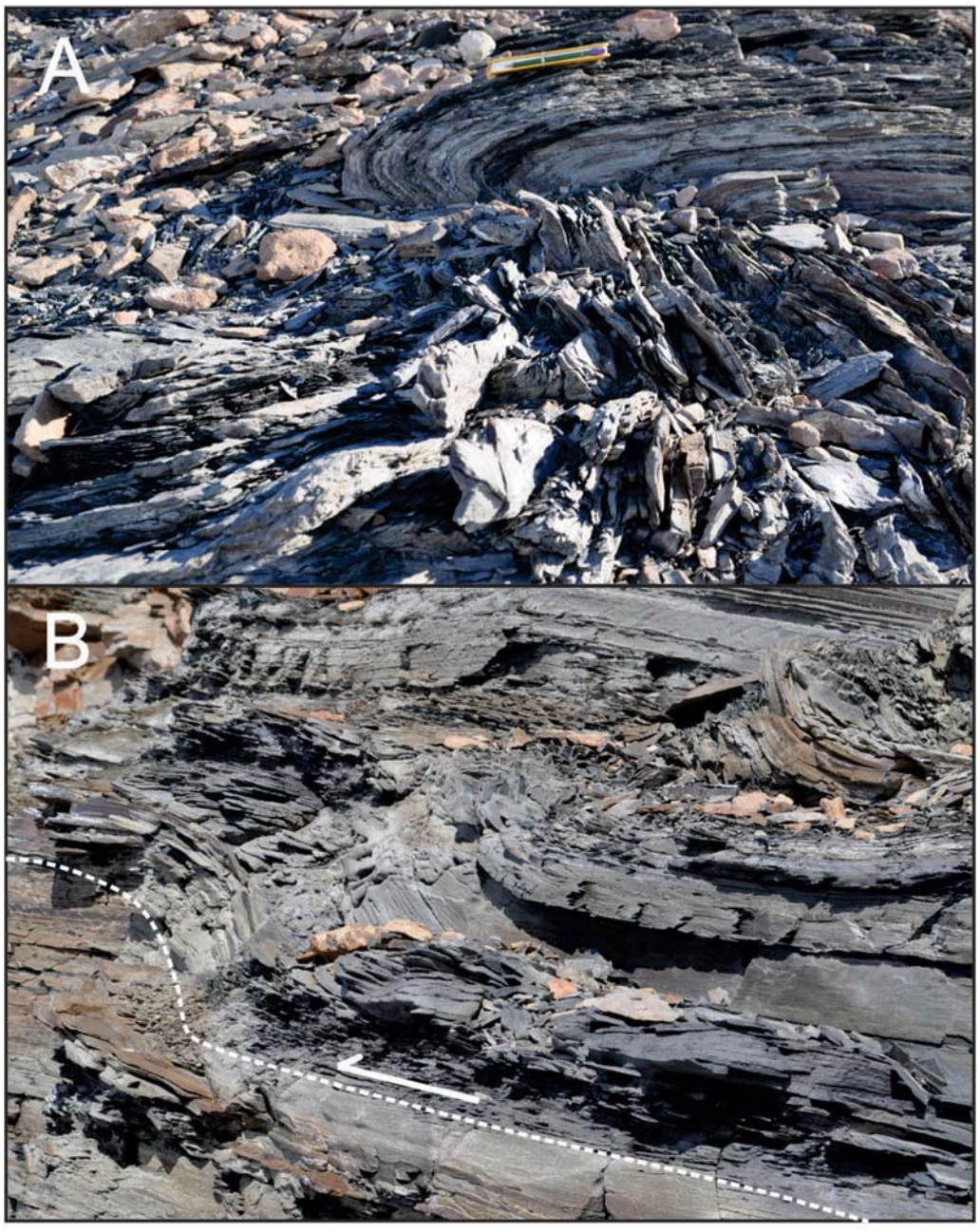

Figure 8. A, Tight, recumbent S-fold in Mackellar beds (site 5, Figure 6). Field notebook for scale (white arrow). **B,** Open Z-fold, which has the appearance of a ramp fold verging south (left); a thrust plane (dashed white line and arrow) underlies the folded beds (site 5, Figure 6). View to the west.

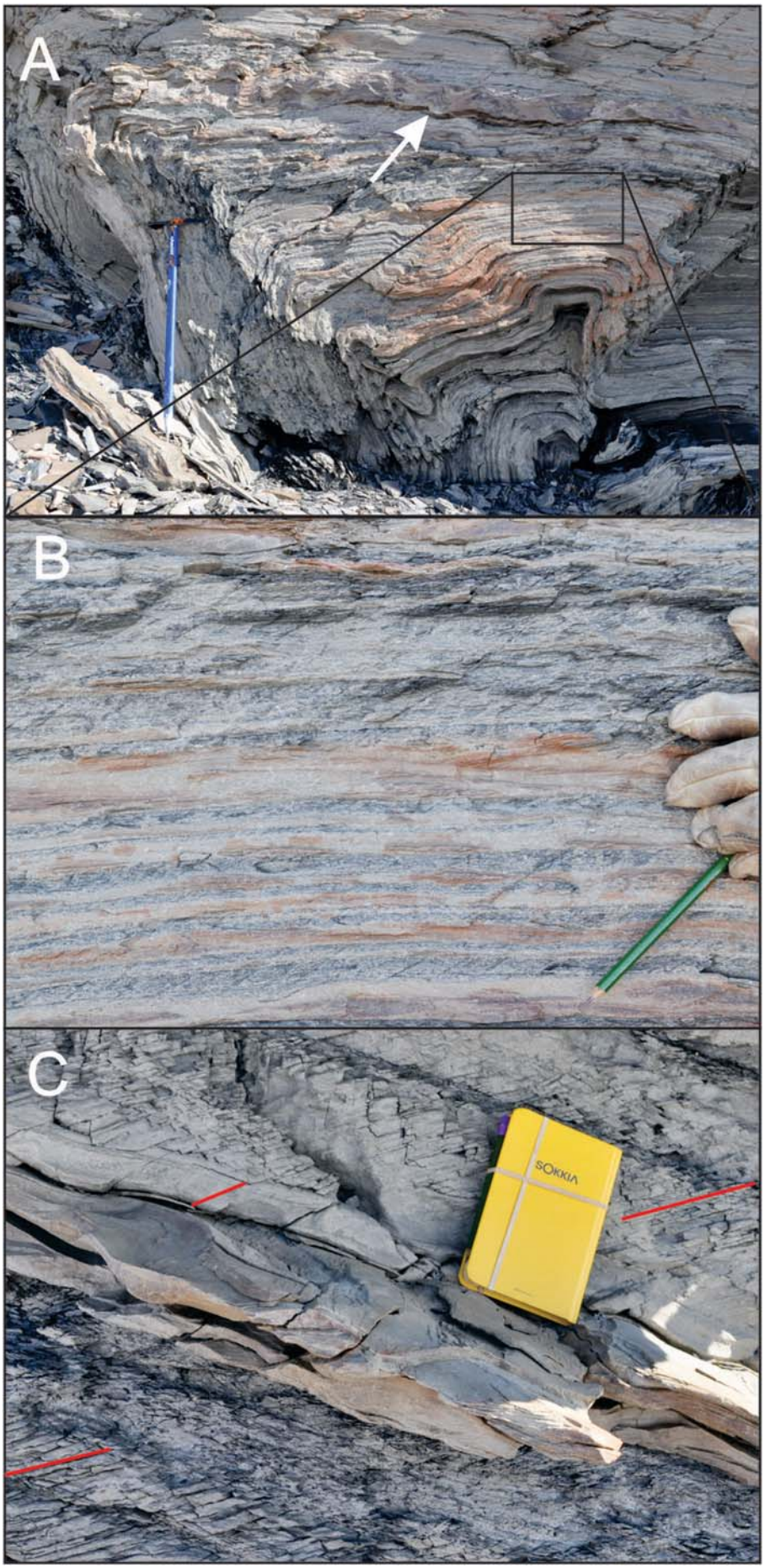

Figure 9. A, Kink bands forming a box fold with S- and Z- forms at various scales (site 10, Figure 6). Note the crumpled sandstone bed (white arrow), which varies in thickness and degree of folding. **B,** Cleavage (spaced and parallel to the pencil) in fine-grained beds, and parallel to fractures and axial planes of folds present at the lower right in A. **C,** Cleavage, indicated by red lines, in beds of slightly different grain sizes (site 14, Figure 6).

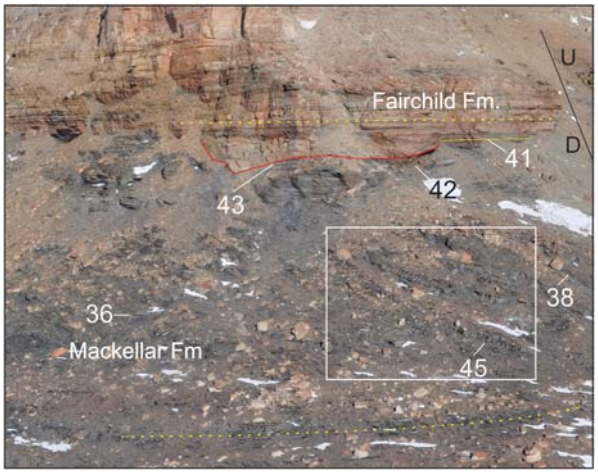

Figure 10. Outcrop south of the fault. Bedding indicated by yellow dashed lines. Designated Mackellar-Fairchild contact marked by solid yellow line. The red line marks, on the left, the channel filled by delta front sandstones and, on the right, the underlying interval of slumped sandstone beds. Sites mentioned in the text and figure captions indicated by white and black numbers. Location of thrust sheets illustrated in Figure 11 are indicated by the white box.

few cases, passes into sandstone beds but is then more widely spaced (Figure 9C).

South of the fault zone

The north–south length of the exposed structure to the south of the fault is about 200 m., and an overview from the southeast is given in Figure 10. The MTD structure is expressed predominantly by thrust sheets that dip gently northwards. A stack of four thrust sheets has been identified at one locality (Figure 11), but they cannot be traced far. Adjacent to the stack of four thrusts, locally beds are folded and cut by thrusts (e.g. Figure 12). Fault breccia is observed along a few thrust planes (Figure 13). The stack of thrusts implies thickening of the Mackellar section, but thickening appears not to be as great as that observed north of the fault zone. The structures here also verge to the south.

The east-facing recessive slope of Mackellar beds passes southward into a southeasterly-facing recessive slope. There, at an angle to the strike of the thrust sheets and folded strata structures in the MTD (thrusts and folds) are impossible to identify with any certainty.

Structure

Attitude measurements were taken on bedding planes (within the MTD and both below and above it), cleavage planes, and fold axes. Variation in the attitudes of the Mackellar beds below the MTD suggest there is an element of slumping; no reliable measurement was obtained, although the overall impression suggests a low westerly dip. Fairchild beds, viewed on the southeast facing outcrop that lies at the southern end of the MTD locality (Figure 3B), appear to have, at most, a westerly dip of only a few degrees. The least uncertain

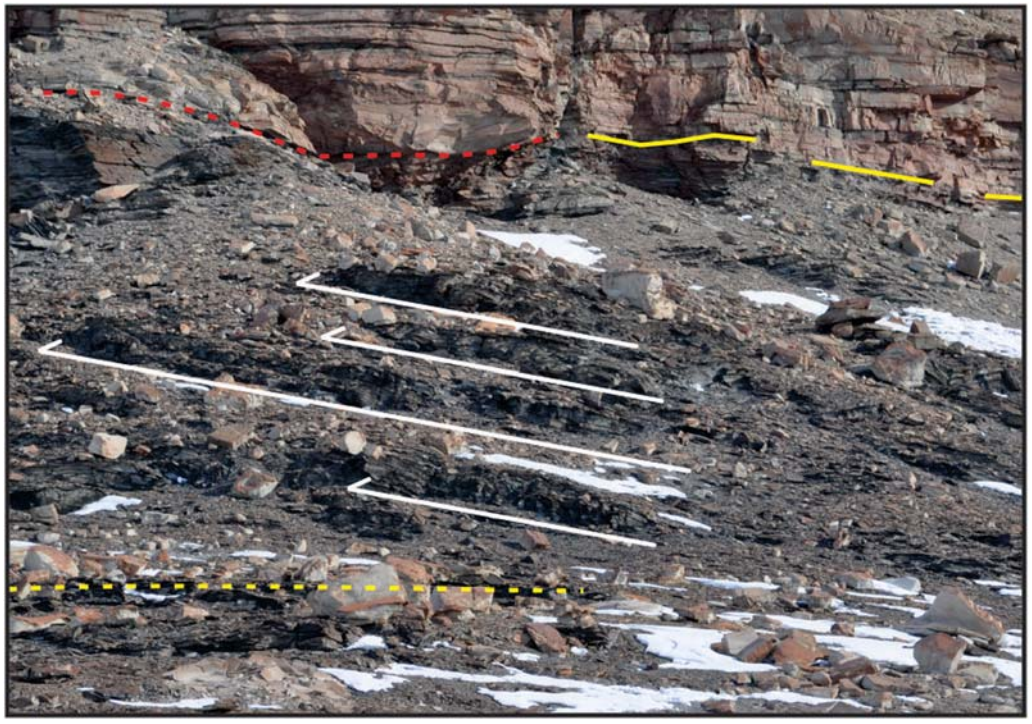

Figure 11. Stack of four thrust sheets in Mackellar beds south of the fault (see Figure 10 for location). Thrust sheet thickness is 2–4 m. Mackellar bedding indicated by dashed yellow line. Solid yellow line marks the base of the undisturbed, continuous Fairchild sandstone beds (perspective leads to the offsets). Dashed red line marks the contact between the Mackellar transition strata and the Fairchild delta beds (see Figure 21).

Figure 12. Deformed strata at the distal (south) end of the exposed mass transport deposit. Buckle fold picked out by the thin brown-weathering sandstone bed. Slight south vergence in the fold is supported by the small displacement thrust (white arrow) cutting the highly contorted thin sandstone bed (site 36, Figure 10). Ice axe at right for scale. View to the west.

measurement of the attitude of the Fairchild Formation is 3° to 247°. Structure contours (Barrett et al. 1970) suggest the Beacon succession has a low westerly dip, although superimposed on this is the possibility of normal faults parallel to the mountain front. The westerly dip has been attributed to Cenozoic uplift and tilting along the Transantarctic Mountains front (Fitzgerald 1994).

Structural analysis of the MTD (Figure 14) demonstrates a mean northerly dip of the bedding, dispersed about a mean sub-horizontal fold axis (trending 3° to 250°), and a slight westerly trend (6° to 253°) of the pole to the bedding plane great circle (π circle). Any correction for the overall attitude of the Mackellar and Fairchild beds makes essentially no difference to either the azimuth of the bedding plane great circle or the trend of the average fold axis. The transport direction based on the top-to-the-south sense of the thrust faults and dominant fold asymmetry (Strachan and Alsop 2006) is taken to be perpendicular to the mean fold axis, i.e. towards c. 160°, which is almost identical to the azimuth (163°) of the bedding plane great circle. Recognising the uncertainties in using slump structures to determine paleoslope orientation (Woodcock 1979), the transport direction is interpreted as the local dip direction of the paleoslope. This is consistent with paleoflow determined from ripple marks and cross-laminations within the Mackellar Formation but outside the zone of deformation, and from nearby stratigraphic sections (Barrett et al. 1986; Isbell et al. 1997; Miller and Collinson 1994).

Cleavage is quite well developed in shaley rocks but only sparsely so in coarser-grained beds (Figure 15). Most Z- and S-fold cleavage measurements (Figure 14) are aligned with bedding; the few outliers might reflect a slightly different stress field. Cleavage fracture in sandstones occurs intermittently and shows little refraction relative to cleavage in adjacent shales. Exposed small scale faults (e.g. Figures 12, 13) all show top to the south.

The principal fault, concealed by talus, is demonstrated by offset of the arbitrarily chosen base of the Fairchild Formation. The offset is about 5 m down to the south (Figures 5, 10). The fault location is constrained by two Mackellar outcrops and two Fairchild outcrops (Figure 16B), which suggest an approximate east–west strike. There is no sign of offset in the underlying Devonian Alexandra Formation and the fault appears not to cut two poorly defined intervals low in the Mackellar beds (Figure 16A). The fault, therefore, is interpreted to be listric, shallowing to the south and resulting from large-scale slumping, rather than the result of tectonism.

Mackellar Formation upper contact

South of the fault zone, the Mackellar/Fairchild contact is gradational and forms a transition zone: over an interval of a few metres, sandstones more typical of the Fairchild Formation are interbedded with shales more typical of the Mackellar Formation. The designated base of the Fairchild Formation is placed at

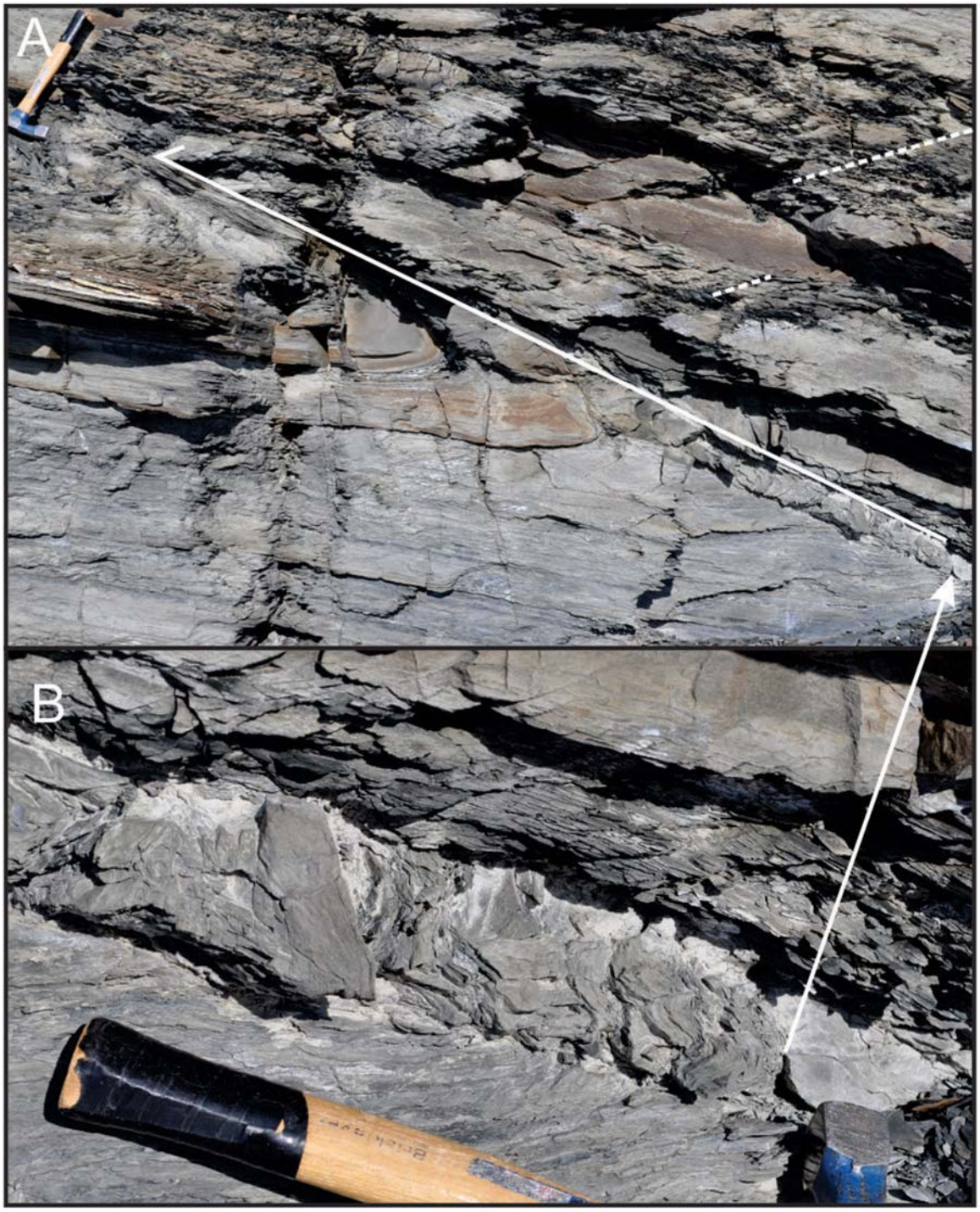

Figure 13. Fault breccia developed along thrust fault plane (site 45, Figure 10). **A,** A thrust parallel to the axial plane of a tight syncline, and displacing the overturned limb. In the coarser-grained bed the thrust is marked by breccia (**B**). Note the cleavage (dashed white lines) in the overlying shale.

the first massive, intact, continuous sandstone bed (Figure 5, Figure 17). Immediately south of the fault zone, there is an irregular interval of strata beneath the interpreted basal Fairchild bed, which consists of broken and displaced slabs and lozenges of sandstone, together with deformed shale (Figure 18A, B). At the southeast nose of the upper Mackellar and lower Fairchild outcrop, this interval is represented by a channel-like filling of sandstone (Figure 10), which overlies a surface cut into shaley beds (Figure 19).

Immediately north of the fault zone, the transition beds consist of interbedded shales and sandstones, similar to those illustrated in Figure 17, and at one exposed contact (site 25, Figure 6), displaced and rotated blocks of sandstone are present below the lowest continuous Fairchild bed (Figure 18C). Projection of the Fairchild basal sandstones to the north suggests that, at the most northerly outcrop, several additional metres of sandstone appear to lie conformably above the Mackellar strata and below the projected Fairchild

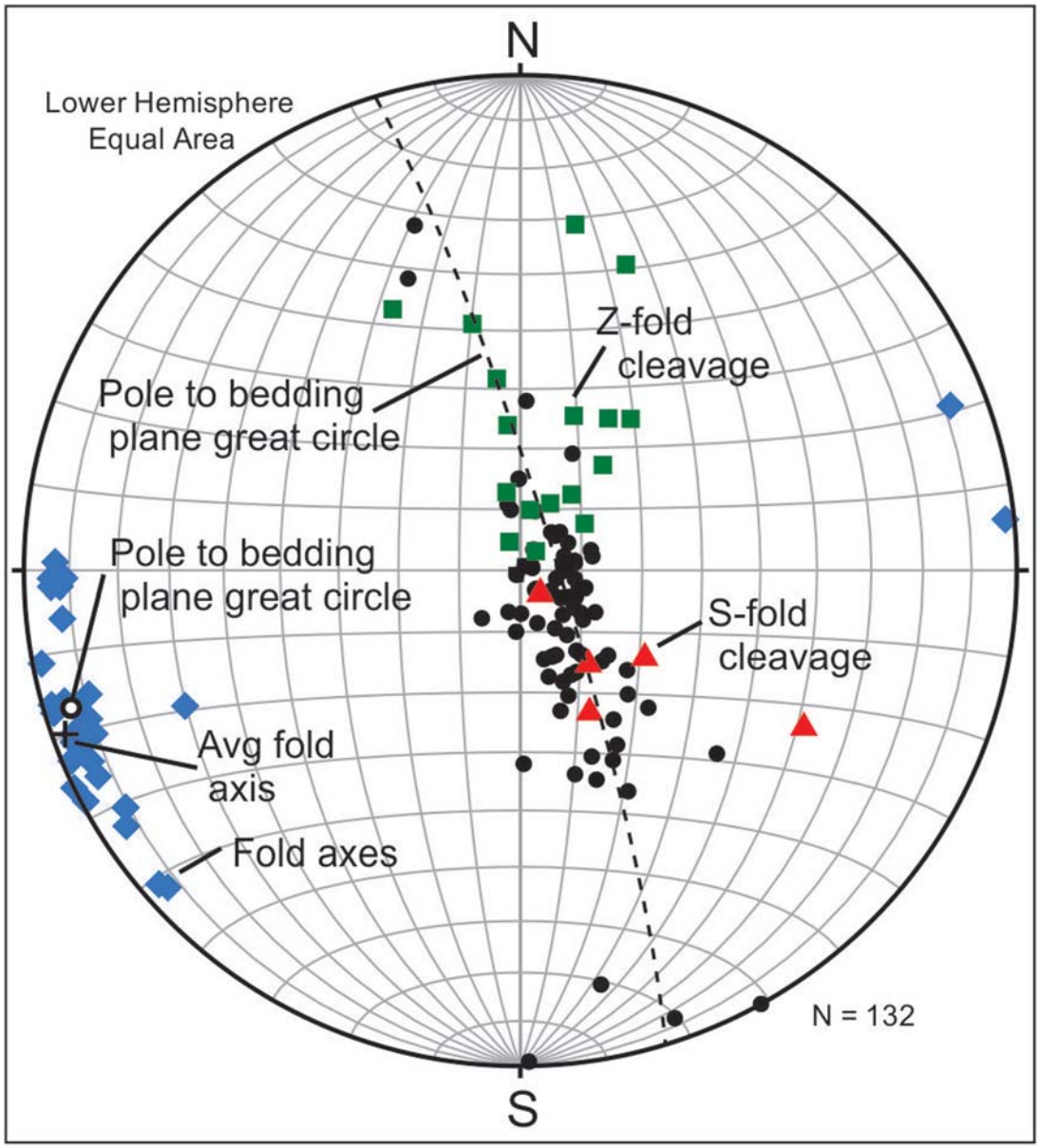

Figure 14. Stereoplot of structural data taken on the MTD. The interpreted transport azimuth and direction is 163°. Symbols: small black dots – poles to bedding planes; black ring – pole to bedding plane great circle; small blue lozenges – fold axes; black cross – average fold axis; small green squares – Z-fold cleavage planes; small red triangles – S-fold cleavage planes.

base (Figure 20). Sandstones in this interval are similar to the Fairchild sandstones and appear to lack the fine-grained interbeds of the transition zone. The interval thins to the south, but unfortunately nowhere is there a continuous section located within this wedge, and therefore it is plausible that fine-grained intervals are concealed beneath the talus. It is not possible to demonstrate either onlap or downlap of these sandstones onto Mackellar beds nor truncation of that wedge interval by the continuous basal Fairchild strata, although the latter possibility seems less probable. However, the Mackellar beds above thrust sheet #4 (site 24, Figure 6) have a low northwesterly dip of 9° to 299° (7° to 340° when corrected using the low westerly plunge, 6° to 253°, of the pole to the MTD bedding plane great circle) and are overlain unconformably by Fairchild sandstones. The increase in dip of these beds below the unconformity is attributed to ramping within the MTD and its doming, which would have lain principally to the southeast.

Discussion

Mass transport deposits vary from blocks which retain their original bedding characteristics (slides) to incoherent masses of sediment in which almost all original features have been destroyed (slumps). The deformational processes range from creep through slide and slump to flow and fall (Posamentier and Martinsen 2011). The principal features of the MTD, folding and thrusting of beds, described here, suggest that it is transitional between a slide and a slump. The instabilities that could have given rise to this MTD include sedimentation, sediment loading, seismic

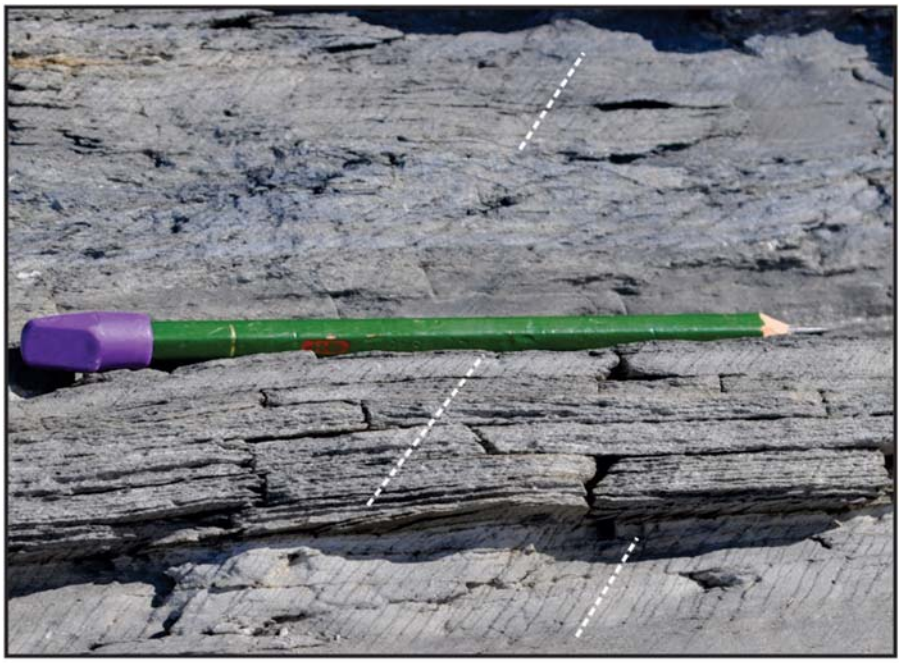

Figure 15. Cleavage, marked by dashed white lines, in beds of varying fine-grain size (site 38, Figure 10).

events and tectonic uplift or tilting (Cossey 2011; Posamentier and Martinsen 2011; Shipp et al. 2011).

Alsop et al. (2017, 2018) showed that cleavage and thrusts were developed in the essentially unlithified deposits of the late Pleistocene (70–15 ka) Lisan Formation in the Dead Sea Basin, Israel. The Lisan beds, which consist of aragonite-rich and detrital-rich laminae, display a wide range of structures. Mackellar strata, in contrast, are laminated to thinly bedded shales to very fine sandstones, and include a prominent sandstone which defines some of the structure (folded beds in thrust sheets 1–6, Figure 6). Structures developed in the Mackellar MTD include S- and Z-folds, which are present at the scale of the thrust sheets, at scales of less than one metre (Figure 9A), and in crumpled sandstone beds (Figure 12) only a few cm thick. Cleavage, including axial plane cleavage, and thrusts at various scales are widely developed. Comparable features are documented in the Lisan Formation and in the Early Pennsylvanian Guandacol Formation in Ischigualasto Provincial Park, San Juan Province, Argentina (Sobiesiak et al. 2017), both of which show that there is no requirement to call on overburden to explain the apparent semi-lithification of the beds (Alsop et al. 2017, 2018; Sobiesiak et al. 2017). Thus, significant sediment cohesion at the time of emplacement of the MTD accounts for the deformation (folding and crumpling) of strata, and the development of cleavage and fault breccia.

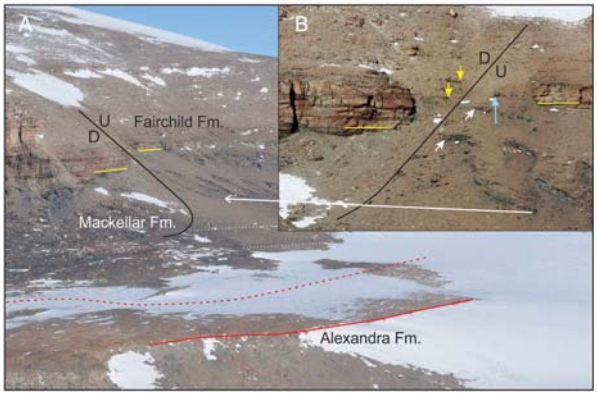

Figure 16. A, Oblique view to illustrate that the fault does not offset the Devonian Alexandra Formation and is therefore a listric fault. Solid red line indicates bedding in the Alexandra strata. Dashed red line marks the approximate position of the upper contact of the Alexandra Formation. A veneer of Pagoda tillite covers the Alexandra Formation. The dashed white lines mark poorly defined bedding in the Mackellar Formation. The solid yellow line marks the top of the transition beds and the designated base of the Fairchild Formation. The fault is interpreted as listric (perspective leads to the sharp bend). **B** (enlarged from Figure 5), The fault must pass between Fairchild sandstone outcrops (yellow arrows) and two sets of Mackellar beds (white arrows) that lie in the fault zone. The small ledge above and to the right of the upper Mackellar outcrop (blue arrow) is interpreted as an interval of interbedded sandstone and finer-grained beds of the Fairchild Formation. The strike of the fault is approximately east-west, with a moderately steep dip to the south at the break in the Fairchild beds. The long white arrow links the two images.

Apart from the thrusting and folding of Mackellar strata, there are a number of facts that bear on interpretation of the structure:

Mackellar Formation

(a) The stratigraphic thickness of the Mackellar Formation increases from the north toward the fault zone

Figure 17. Designated lower contact of the Fairchild Formation (placed at the base of the lowest continuous, intact, sandstone bed) is indicated by a yellow line (site 41, Figure 10). On the left of the image, beds below inferred contact consist of alternating sandstones and shales of the transition zone; on the right, beds below the contact are sheared and displaced (see Figure 18B).

(b) The dip of the thrust sheets increases from the north toward the fault zone.
(c) A little north of the fault zone the upper Mackellar strata are overlain unconformably by Fairchild beds.
(d) The interval of interbedded sandstones and shales designated as the transition beds and marking the changes from the shaley Mackellar Formation to the sandy Fairchild Formation are, in places, broken, displaced, and rotated.
(e) From near the fault zone northwards a wedge-shaped interval, below the lowest continuous Fairchild bed, consists predominantly of sandstones.

The MTD in the Mackellar Formation north of the fault zone is most obviously expressed in the folds and thrusts that form an isolated belt of strata in the middle of the succession. It is bounded below and above by intervals of undisturbed beds, which are, for the most part, covered in talus. South of the fault zone the large-scale folds and thrust sheets are replaced by smaller thrusts sheets (Figure 11) and folds (Figure 12) that differ in scale from most of those north of the fault zone. The possibility that the very different structures seen on either side of the fault zone were generated in entirely separate events is regarded as highly improbable.

The apparent increase in thickness of the Mackellar beds from the north toward the fault zone together with the increasing dip of the upper, *in situ*, Mackellar beds (Figure 20) suggests that the Mackellar beds were domed and at a later stage truncated, which resulted in the unconformable relationship with Fairchild strata (site 24, Figure 6).

The basal Fairchild strata are a significant part of the development of the field relations as seen today. North of the fault zone the wedge of sandstones is interpreted as a proximal delta front, prograding channel mouth bars, and terminal distributary channels of a delta. These wedge beds are interpreted as downlapping foresets deposited on Mackellar strata. They appear to thin toward the south, although without paleocurrent data the orientation of the delta front remains unknown. The alternative that the wedge beds onlap the Mackellar strata is certainly possible because of the doming above the MTD. South of the fault zone, the Fairchild strata are interpreted as a deltaic succession (Figure 21), which includes a prominent channel fill (Figures 10, 19). Immediately north of the fault zone (site 24, Figure 6) and also to its south (Figure 17), transition beds display rotated and displaced sandstone lozenges and sheets (Figure 18). These are interpreted as slumped but cohesive sandstone bodies, such as have been observed elsewhere in deltaic sequences (Sobiesiak et al. 2017; Strachan and Alsop 2006).

Fault zone

(a) The basal Fairchild beds are offset vertically and separated laterally across a fault, but no offset is apparent in the Devonian Alexandra Formation.
(b) Within the fault zone, where basal Fairchild beds are almost entirely absent, isolated outcrops of Mackellar strata are similar to those in thrust sheets north of the fault zone.
(c) Field relations in the fault zone demonstrate an extensional structure.

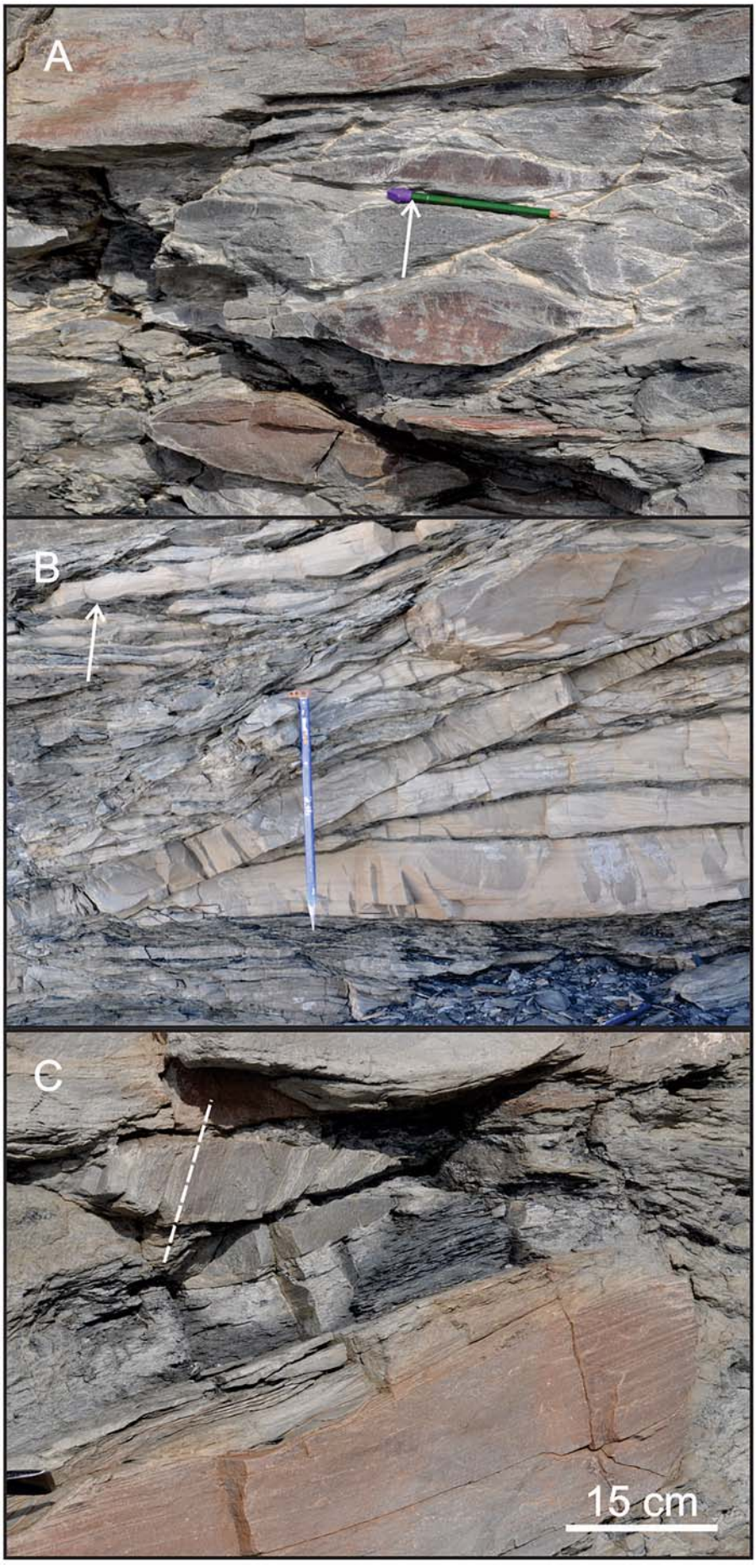

Figure 18. A, Sandstone 'lozenges' separated by shear planes (site 41, Figure 10). Pencil (white arrow) for scale. **B,** Sheared and displaced sandstone blocks in the transition interval between the Mackellar shales and the designated base of the Fairchild Formation (site 42, Figure 10). In the upper part of the image, a several-centimetre thick sandstone (white arrow) exhibits boudinage. Ice axe for scale. **C,** Rotated block of sandstone with bedding indicated by dashed white line (site 25, Figure 6).

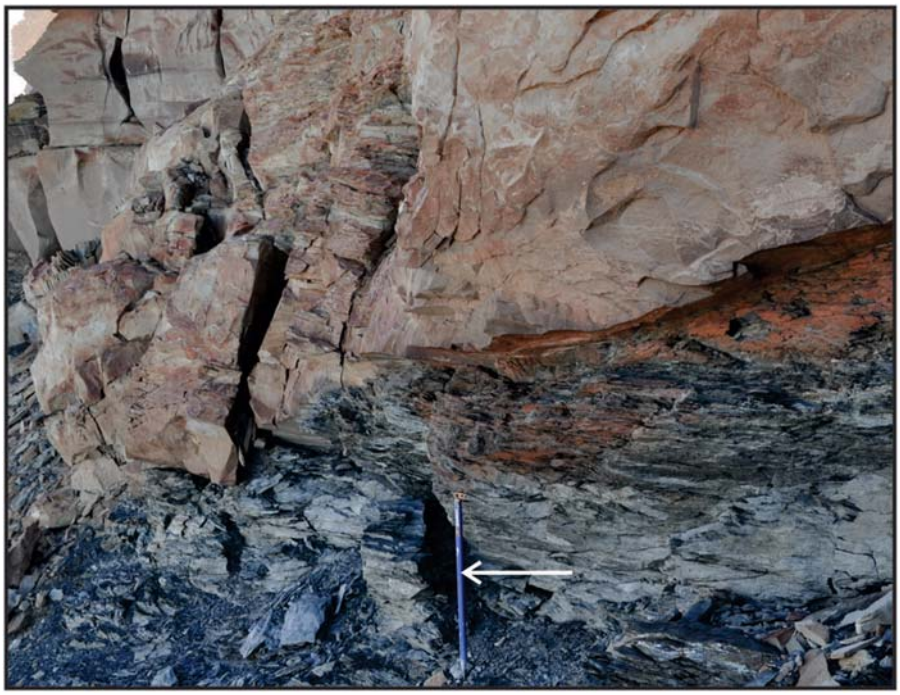

Figure 19. Contact relations of the channel fill illustrated in Figure 10 (site 43, Figure 10). Scale given by ice axe (arrow).

The scattered outcrops in the fault zone define, approximately, a moderately steep south-dipping fault, which must be listric because it does not offset the Devonian Alexandra Formation. This fault must post-date the early stages of Fairchild deposition, and suggests that loading by Fairchild sandstones was the probable cause. Nevertheless, neither Fairchild nor Mackellar beds south of the fault zone show the back rotation that is commonly seen with such movements. Further, apart from sheared shaley beds below the Fairchild delta south of the fault zone, there is no deformation in the Mackellar beds that might be attributed to thinning of the Mackellar succession as a result of the approximate five metre downward displacement of the Fairchild strata, although poor exposure might explain this issue.

Interpretation

The structural data demonstrate that the MTD moved to the south-southeast (c. 163°). The MTD occurred towards the head of a low-lying inland sea (Mackellar Sea), moving down a slope with a very shallow dip. The driving mechanism was probably gravitational loading of a section of Mackellar beds. Alternatively, the MTD might have resulted from tectonism, either earthquake activity or tectonic uplift and slight tilting in the source region, which destabilised a mass of Mackellar beds.

A tentative history of the development of the field relations observed at the MTD locality is presented here. Glacial beds of the Pagoda Formation were deposited on a local paleotopographic high on the

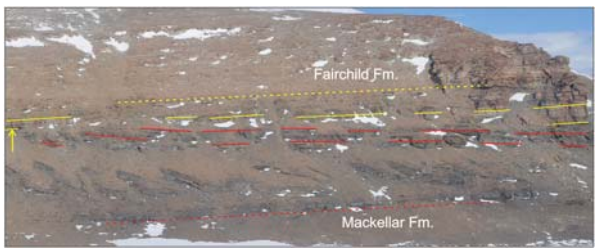

Figure 20. Apparent attitudes of bedding to illustrate the sediment wedge from the bluff at the north end of the outcrop (right) southward to near the fault zone (left). Yellow arrow (on left) marks the base of the first continuous Fairchild sandstone, and immediately to the right (north), attitudes (indicated by solid red and yellow lines) suggest an angular discordance. Solid lines indicate bedding planes. Dashed red and yellow lines indicate the larger scale bedding attitudes.

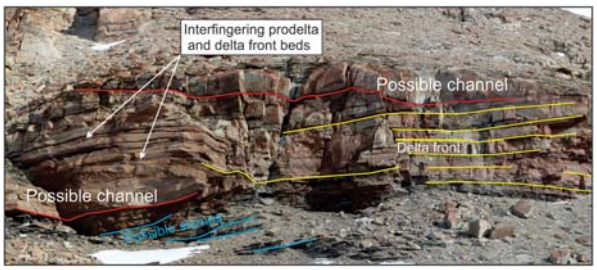

Figure 21. Deltaic succession south of fault and located above site 42, Figure 10. Interfingering deltaic sandstones and prodelta shales are sandwiched between Mackellar shales and more massive Fairchild sandstones at the bluff south of the fault (Figure 10). At the left of the image, possible slumped Mackellar beds occur at the base of a massive sandstone. Another possible channel caps the bluff.

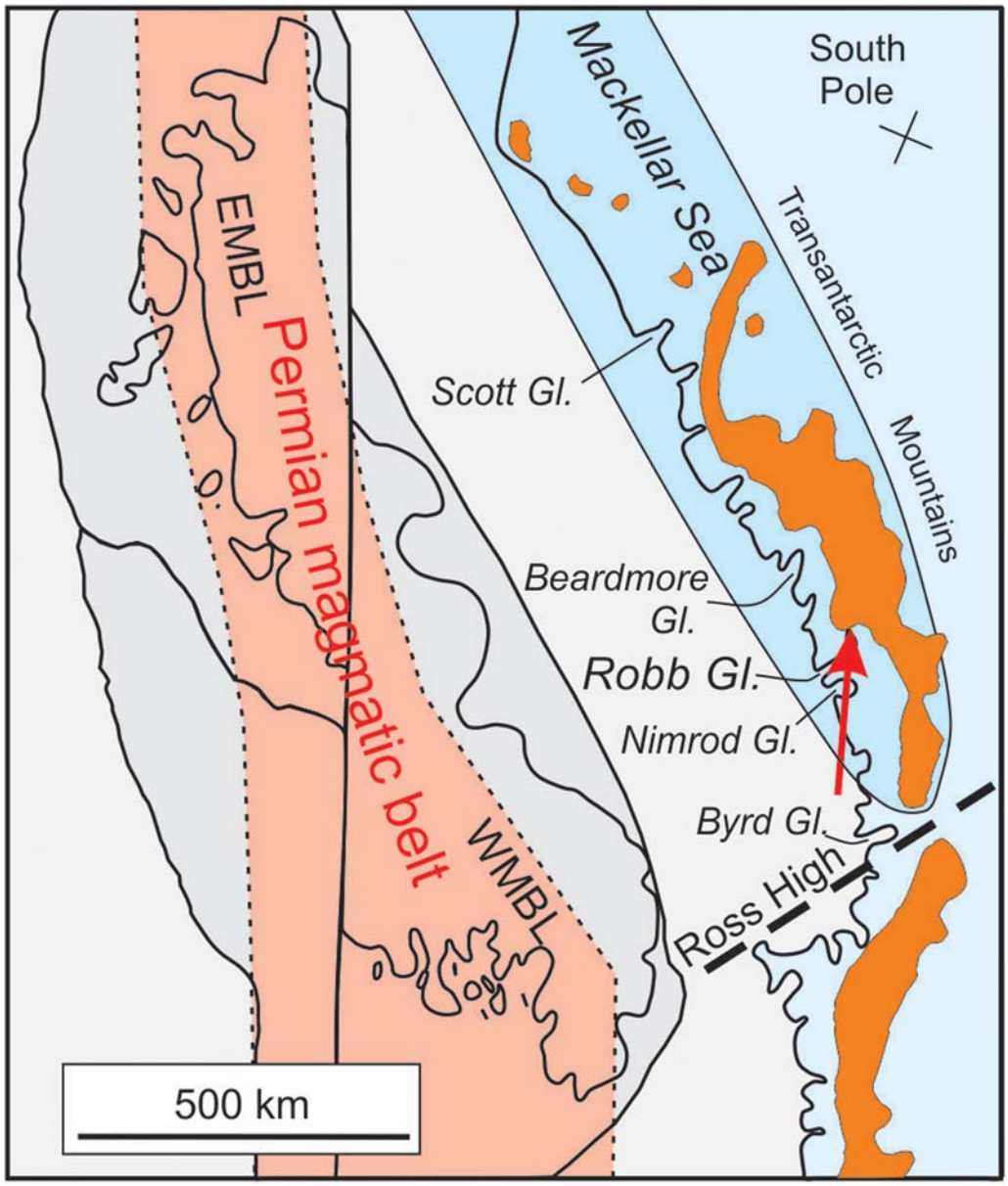

Figure 22. The Permian Gondwana margin of Antarctica superimposed on present-day geography, but with post-break-up extension in the Ross embayment removed, which brings the Permian magmatic belt much closer to the Transantarctic Mountains (EMBL: eastern Marie Byrd Land; WMBL: western Marie Byrd Land). The position and components of the Permian magmatic belt are taken from Elliot et al. (2017). The Mackellar Sea (in deeper blue) was inland of the plate margin and opened to the Panthallassic Ocean in the region of the Antarctic Peninsula. Extant Permian outcrops indicated in orange. The Ross High separated the south Victoria Land Beacon succession from the Mackellar Sea. The red arrow marks the location and orientation of the MTD transport direction.

Maya Erosion Surface. Only a thin veneer, possibly a dropstone facies deposited late in Pagoda time, is present. The contact with the Mackellar Formation is not exposed. A few tens of metres of shales, silts and fine-grained sands were deposited, but included a few discontinuous beds of coarser-grained sand, seen low in the section south of the fault zone and more prominently north of the fault zone preserved as a single relatively thick bed within the MTD thrust slices. The MTD, probably activated by gravitational loading, moved southward an unknown distance until brought to a halt by a backstop located south of the extant outcrops.

The result in the toe region south of the fault zone was thrusting and local folding of essentially homogenous beds. A set of four c. 2- to 4-m-thick thrust sheets form a recognisable stack, and other thrust sheets appear to be present south of that stack. At least one thin sandstone shows spectacular folding, crumpling and slight thrust displacement (Figure 12), and folds on a somewhat larger scale also occur (north of the thrust stack and below site 42, Figure 10). The location of the backstop jumped northward, and north of the fault zone the main body of the MTD was created. Close to the new backstop, inferred to be in the fault zone, the Mackellar strata

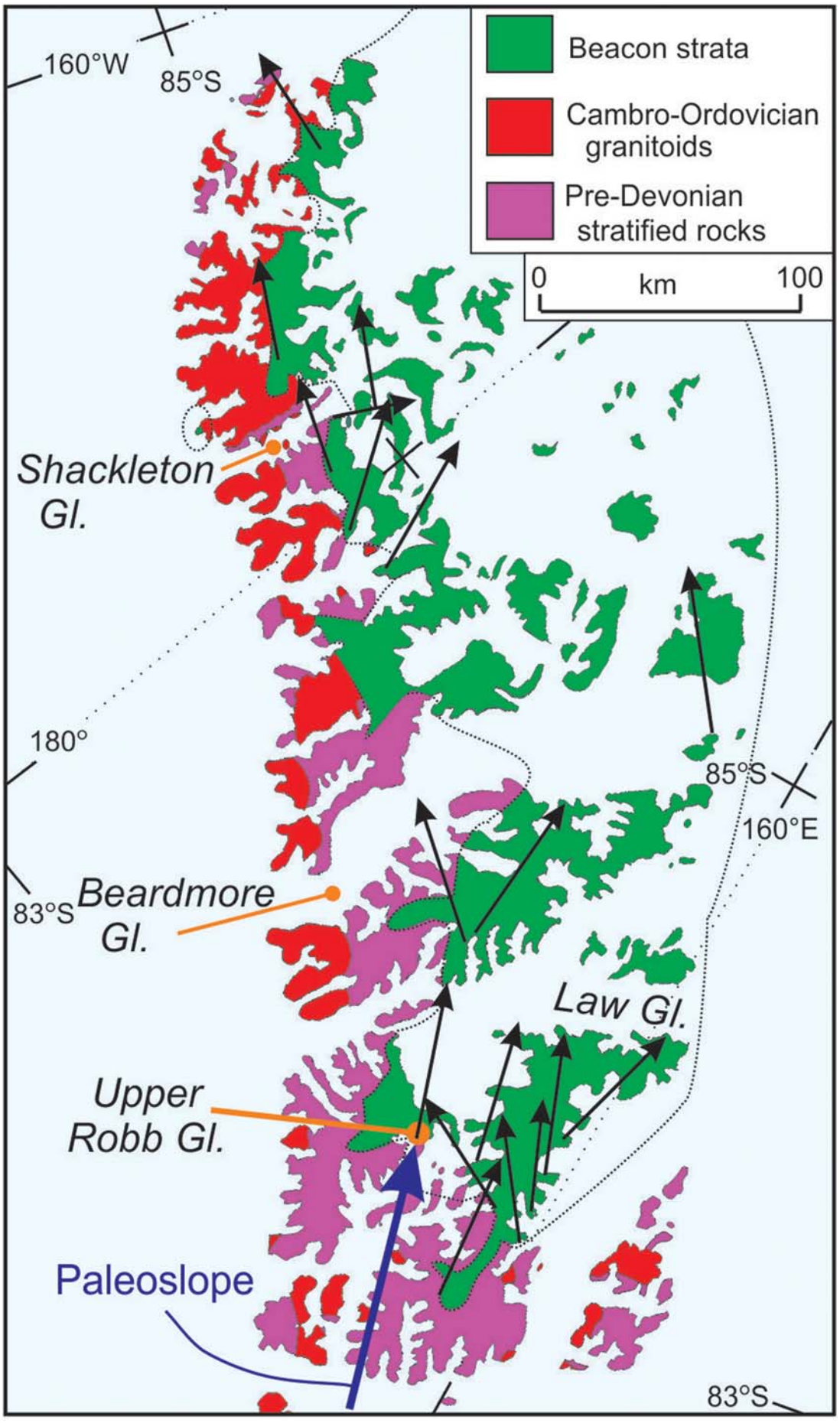

Figure 23. Paleocurrent directions, from current ripple marks and cross-laminations, in the Mackellar Formation in black with the tails of arrows on the measurement sites. The mass transport deposit azimuth, from the stereoplot, in dark blue with the head of the arrow on the measurement site (upper Robb Glacier). Data sources: (Barrett et al. 1986; Isbell et al. 1997; Miller and Collinson 1994).

were folded and then cut by thrusts back-stepping successively away from the toe region. The folds are recorded mainly by hinges; no thrust-parallel inverted limbs are preserved suggesting that the thrusts cut through tight small-scale folds which lacked long inverted limbs. Only one thrust sheet (thrust sheet 6, Figure 6) includes a strongly deformed sandstone bed, which defines an upright fold.

Deposition of fine-grained beds then continued with the accumulation of several tens of metres of sediment, now partly hidden by talus but exposed as the upper *in situ* Mackellar beds. Immediately thereafter, the MTD north of the fault zone was reactivated but moved southward only a short distance. However, this reactivation caused the steepening of the thrust sheets, with the consequent thickening and doming of the Mackellar section, and resulted in the anomalous dip of the beds at Site 25 (Figure 6). This dome, with a steeper southern flank, constituted the paleotopography at the start of deltaic sedimentation. The sedimentation is recorded initially as the designated transition beds, which comprise interbedded Mackellar and Fairchild lithologies.

Increasing paleocurrent velocity associated with hyperpycnal flow down the delta fronts winnowed off most of the dome of Mackellar strata. North of the dome, an advancing delta front deposited the wedge beds, and at the same time a little to the south (site 24, Figure 6) another advancing delta front resulted in transition beds. This delta front, early in its history, was unstable and slumped, leading to the rotated blocks such as observed at site 24 (Figures 6, 18C). This delta front was most probably part of a larger feature that is recorded south of the fault zone (Figure 21), where the transition beds also exhibit slump features (Figure 18B). A little farther south, this delta front shows slumped slabs of cohesive sandstone, overlain by the build-up of the delta as a series of sandstone lobes. The base of the delta is marked by a prominent channel, possibly a terminal distributary channel, cut into Mackellar beds (Figures 10, 19). Eventually deltaic sedimentation in the form of distal delta front, delta mouth bars, and terminal distributary channels (cf. Flaig et al. 2016) filled paleotopography on the Mackellar beds and continuous sheets of sandstone were deposited across the whole of the now-buried MTD.

Sedimentation of the Fairchild Formation continued but after some interval of time the load of the thicker deltaic succession south of the fault was sufficient to cause gravitational collapse, dropping the Fairchild and underlying transition beds about five metres along a listric fault. The fault, where it crosses the basal Fairchild beds, has a moderately steep dip to the south but is inferred to flatten out to the south within the Mackellar beds.

Regional setting

The elongate Mackellar Sea narrowed and diminished northward (present co-ordinates) toward the Ross High where there was spatial convergence with the Permian plate margin (Figure 22). The Mackellar Formation was deposited in a rift enclosing an elongate marine/brackish/lacustrine basin oriented sub-parallel to the present mountain range, and with axial drainage to the south-southeast (present co-ordinates) (Isbell 2015; Isbell et al. 1997, 2008). The MTD originated on a shallow slope rising toward the elevated Ross High terrain (Collinson et al. 1994) that separated the Victoria Group basin in the central Transantarctic Mountains from that in south Victoria Land. Because of spatial separation from the Ross High, the MTD probably originated from a closer location. Although MTDs do not necessarily flow down paleoslope, the transport direction is consistent with paleocurrent orientations derived from current ripple marks and cross-laminations in the Mackellar Formation in the Queen Elizabeth and Queen Alexandra ranges (Figure 23; Barrett et al. 1986; Miller and Collinson 1994; Isbell et al. 1997), and suggests additional evidence for paleoslope orientation.

Given that the Gondwana plate margin and magmatic arc were active during the early Permian (Elliot et al. 2017), the trigger mechanism could have been any combination of tectonic uplift along the plate margin leading to instability in the Mackellar basin fill, earthquake activity, and simple gravitational loading possibly coupled with local relief created by delta progradation.

Data availability statement

The data that support the findings of this study are available from the corresponding author (DHE), upon reasonable request.

Acknowledgments

Work in the field was made possible by the helicopter support provided by Petroleum Helicopters Inc. and by Raytheon Polar Services. Sam Hulett provided much field assistance. Shelley Judge gave significant assistance with the stereoplot. Reviews by Nigel Woodcock and Ian Alsop are much appreciated. Byrd Polar and Climate Research Center contribution number 1601.

Disclosure statement

No potential conflict of interest was reported by the author(s).

Funding

Fieldwork was supported by National Science Foundation grants (ANT 0944662 to DHE and ANT 0838851 to JLI).

ORCID

David H. Elliot http://orcid.org/0000-0002-6111-0508

References

Alsop GI, Marco S, Levi T, Weinberger R. 2017. Fold and thrust systems in Mass Transport Deposits. Journal of Structural Geology. 94:98–115.

Alsop GI, Weinberger R, Marco S. 2018. Distinguishing thrust sequences in gravity-driven fold and thrust belts. Journal of Structural Geology. 109:99–119. doi:10.1016/j.jsg.2018.01.005.

Alsop GI, Weinberger R, Marco S, Levi T. 2019. Identifying soft-sediment deformation in rocks. Journal of Structural Geology. 108:1–8. doi:10.1016/j.jsg.2017.09.001.

Ammerman R, Nelson EP, Gardner MH, Trudgill B. 2011. Submarine mass-transport deposits of the Permian Cutoff Formation, West Texas, U.S.A.: internal architecture and controls on overlying reservoir sand deposition. In: Shipp RC, Weiner P, Posamentier HW, editors. Mass-transport deposits in deep-water Settings. Vol. 96. Tulsa, Oklahoma: Society of Economic Paleontologists and Mineralogists Special Publication; p. 235–267.

Barrett PJ. 1968. The post-glacial Permian and Triassic Beacon rocks in the Beardmore Glacier area, central Transantarctic Mountains, Antarctica. [PhD dissertation]. Ohio State University, Columbus, Ohio 510 pp.

Barrett PJ. 1991. The Devonian to Triassic Beacon Supergroup of the Transantarctic Mountains and correlatives in other parts of Antarctica. In: Tingey RJ, editor. The geology of Antarctica. Oxford Monographs on Geology and Geophysics. Vol. 17. Oxford: Oxford University Press; p. 120–152.

Barrett PJ, Elliot DH, Lindsay JF. 1986. The Beacon Supergroup (Devonian-Triassic) and Ferrar Group (Jurassic) in the Beardmore Glacier area, Antarctica. In: Turner MD, Splettstoesser JF, editors. Geology of the central Transantarctic Mountains. Vol. 36. Washington, DC: American Geophysical Union, Antarctic Research Series; p. 339–428.

Barrett PJ, Lindsay JF, Gunner J. 1970. Reconnaissance geologic map of the Mount Rabot Quadrangle, Transantarctic Mountains, Antarctica. United States Geological Survey, Antarctic Map No 1, 1:250 000.

Collinson JW, Elliot DH, Isbell JL, Miller JMG. 1994. In: Veevers JJ, Powell CMcA, editors. Permian-Triassic Transantarctic Basin, Permian-Triassic Pangean Basins and Foldbelts along the Panthalassan margin of Gondwanaland. Geological Society of America Memoir. 184:173–222.

Cossey SPJ. 2011. Mass-transport deposits in the Upper Paleocene Chicontepec Formation, Mexico. In: Shipp RC, Weiner P, Posamentier HW, editors. Mass-transport deposits in deep-water settings. Vol. 96. Tulsa, Oklahoma: Society of Economic Paleontologists and Mineralogists Special Publication; p. 269–277.

Dykstra M, Garyfalou K, Kertznus V, Kneller B, Milana JP, Molinaro M. 2011. Mass-transport deposits: combining outcrop studies and seismic forward modeling to understand lithofacies distributions, deformation, and their seismic stratigraphic expressions. In: Shipp RC, Weiner P, Posamentier HW, editors. Mass-transport deposits in deep-water settings. Vol. 96. Tulsa, Oklahoma: Society of Economic Paleontologists and Mineralogists Special Publication; p. 293–310.

Elliot DH. 2013. The geological and tectonic evolution of the Transantarctic Mountains: a review. In: Hambrey MJ, Barker PF, Barrett PJ, Bowman V, Davies B, Smellie JL, Tranter M, editors. Antarctic palaeoenvironments and earth-surface processes. Vol. 381. Geological Society of London Special Publication; p. 7–35. doi:10.1144/SP381.14.

Elliot DH, Fanning CM, Isbell JL, Hulett SRW. 2017. The Permo-Triassic Gondwana sequence, central Transantarctic Mountains, Antarctica: zircon geochronology, provenance, and basin evolution. Geosphere. 13:155–178. doi:10.1130/GES01345.1.

Fitzgerald PG. 1994. Thermochronologic constraints on post-Paleozoic tectonic evolution of the central Transantarctic Mountains, Antarctica. Tectonics. 13:634–662.

Flaig PP, Hasiotis ST, Jackson AM. 2016. An Early Permian, palaeopolar, postglacial, river-dominated deltaic succession in the Mackellar-Fairchild formations at Turnabout Ridge, central Transantarctic Mountains, Antarctica. Palaeogeography, Palaeoclimatology, Palaeoecology. 441:241–265. doi.org/10.1016/j.palaeo.2015.08.004.

Ineson J. 1985. Submarine glide blocks from the Lower Cretaceous of the Antarctic Peninsula. Sedimentology. 32:659–670.

Isbell J. 1999. The Kukri Erosion Surface; a reassessment of its relationship to the rocks of the Beacon Supergroup in the central Transantarctic Mountains, Antarctica. Antarctic Science. 11:228–238.

Isbell JL. 2015. Permian and Triassic sedimentation in the central Transantarctic Mountains, southern Victoria Land and northern Victoria Land: a south polar view of Gondwana during the Paleozoic-Mesozoic transition. 21st International Symposium on Polar Sciences, Korean Polar Research Institute, Incheon, Republic of Korea, Abstracts with Programs. p. 32–35.

Isbell JL, Koch ZJ, Szablewski GM, Lenaker PA. 2008. Permian glacigenic deposits in the Transantarctic Mountains, Antarctica. In: Fielding CR, Frank TD, Isbell JL, editors. Resolving the late Paleozoic ice age in time and space. Vol. 441. Boulder (CO): Geological Society of America Special Paper; p. 59–70.

Isbell JL, Seegers GM, Gelhar GA. 1997. Upper Paleozoic glacial and post-glacial deposits, central Transantarctic Mountains, Antarctica. In: Martini IP, editors. Late glacial and postglacial environmental changes: Quaternary, Carboniferous-Permian, and Proterozoic. Oxford: Oxford University Press; p. 230–242.

King PR, Ilg BR, Arnot M, Browne GH, Strachan LJ, Crundwell M, Helle K. 2011. Outcrop and seismic examples of mass-transport deposits from a late Miocene deep-water succession, Taranaki Basin, New Zealand. In: Shipp RC, Weiner P, Posamentier HW, editors. Mass-transport deposits in deep-water settings. Vol. 96. Tulsa, Oklahoma: Society of Economic Paleontologists and Mineralogists Special Publication; p. 235–267.

Laird MG, Mansergh GD, Chappell JMA. 1971. Geology of the central Nimrod Glacier area, Antarctica. New Zealand Journal of Geology and Geophysics. 14:427–468.

Macdonald DIM, Moncrieff ACM, Buttterworth PJ. 1993. Giant slide deposits from a Mesozoic fore-arc basin, Alexander Island, Antarctica. Geology. 21:1047–1050.

Miller MF, Collinson JC. 1994. Late Paleozoic post-glacial inland sea filled by fine-grained turbidites: Mackellar Formation, central Transantarctic Mountains. In:

Deymoux M, Miller JMG, Domack EW, Eyles N, Fairchild IJ, Young GM, editors. The earth's glacial record. Cambridge: Cambridge University Press; p. 215–233.

Miller MF, Isbell JL. 2010. Reconsrtruction of a high-latitude, post-glacial lake: Mackellar Formation (Permian), Transantarctic Mountains. In: López-Gamundí OR, Buatois LA, editors. Late paleozoic glacial events and post-glacial transitions in Gondwana. Vol. 468. Geological Society of America, Special Papers; p. 193–207. doi:10/1130/20102468(09).

Moscardelli L, Wood L, Mann P. 2006. Mass-transport complexes and associated processes in the offshore area of Trinidad and Venezuela. American Association of Petroleum Geologists Bulletin. 90:1059–1088.

Posamentier HW, Martinsen OJ. 2011. The character and genesis of submarine mass-transport deposits: insights from outcrop and 3D seismic data. In: Shipp RC, Weiner P, Posamentier HW, editors. Mass-transport deposits in deep-water settings. Vol. 96. Tulsa, Oklahoma: Society of Economic Paleontologists and Mineralogists Special Publication; p. 7–38.

Posamentier HW, Walker RG. 2006. Deep water turbidites and submarine fans. In: Posamentier HW, Walker RG, editors. Facies models revisited. Vol. 84. Tulsa, Oklahoma: Society of Economic Paleontologists and Mineralogists Special Publication; p. 397–520.

Shipp RC, Weimer P, Posamentier HW, editors. 2011. Mass-transport deposits in deepwater settings. Tulsa (OK): SEPM (Society of Sedimentary Geology). p. 510.

Sobiesiak MS, Alsop GI, Kneller B, Milana JP. 2017. Subseismic scale folding and thrusting within an exposed mass transport deposit: a case study from NW Argentina. Journal of Structural Geology. 96:176–191.

Strachan LJ, Alsop GI. 2006. Slump folds as estimators of palaeoslope: a case study from the Fisherstreet Slump of County Clare, Ireland. Basin Research. 18:451–470.

Stump E. 1995. The Ross orogen of the Transantarctic Mountains. Cambridge: Cambridge University Press. p. 284.

Van der Merwe WC, Hodgson DM, Slint SS. 2009. Widespread syn-sedimentary deformation on a muddy deep-water basin-floor: the Vischkuil Formation (Permian), Karoo, South Africa. Basin Research. 21:289–406.

Woodcock NH. 1979. The use of slump structures as palaeoslope orientation estimators. Sedimentology. 26:83–99.